Lipidomics of *Thalassiosira pseudonana* Under Phosphorus Stress Reveal Underlying Phospholipid Substitution Dynamics and Novel Diglycosylceramide Substitutes

Running Title: P-Stress Diatom Lipidomics

Jonathan E. Hunter[1,2†], Joost Brandsma[3], Marcus K. Dymond[4], Grielof Koster[3], C. Mark Moore[1], Anthony D. Postle[3], Rachel A. Mills[1] and George S. Attard[5].

1. Ocean and Earth Science, University of Southampton, National Oceanography Centre Southampton, European Way, Southampton, SO14 3ZH, United Kingdom
2. Institute for Life Sciences, University of Southampton, SO17 1BJ, United Kingdom
3. Faculty of Medicine, University of Southampton, Southampton General Hospital, Tremona Road, Southampton, SO16 6YD, United Kingdom
4. Division of Chemistry, School of Pharmacy and Biomolecular Sciences, University of Brighton, Brighton, BN2 4GJ, United Kingdom
5. Chemistry, University of Southampton, Southampton, SO17 1BJ, United Kingdom

†Corresponding Author: jhunter@whoi.edu; Current Address: Marine Chemistry and Geochemistry, Woods Hole Oceanographic Institution, Woods Hole, MA 02543-1050, United States of America

Abstract

Phytoplankton substitute phosphorus (P) containing lipids with non-P analogues boosting growth in P-limited oceans. In the model diatom *Thalassiosira pseudonana*, lipid headgroup substitution dynamics are well described, but those of the individual lipids, varying in fatty acids, are unknown. Moreover, the behaviour of lipids outside of the common headgroup classes, and the relationship between lipid substitution and cellular particulate organic P (POP) are yet to be reported. We investigated these through the mass spectrometric lipidomics of P replete (P+) and depleted (P-) *T. pseudonana* cultures. Non-lipidic POP was depleted rapidly by the initiation of P stress, followed thereafter by cessation of P-lipid biosynthesis and per-cell reduction in P-lipid of successive generations. Minor P-lipid degradative breakdown was observed, releasing P for other processes, but most remained intact. This may confer an advantage to efficient heterotrophic lipid consumers in P limited oceans. Glycerophosphatidylcholine (PC), the predominant P-lipid, was similar in composition to its betaine substitute lipid. During substitution, PC per cell was less abundant and more highly unsaturated in composition. This may reflect underlying biosynthetic processes or the regulation of membrane biophysical properties subject to lipid substitution. Finally, several diglycosylceramide lipids increased up to ten-fold under P stress. These represent novel substitute lipids and potential biomarkers for the study of P limitation in situ, contributing to growing evidence highlighting the importance of sphingolipids in phycology. These findings contribute deeply to our understanding of P-lipid substitution, a powerful and widespread adaptation to P limitation in the oligotrophic ocean.

43 **Importance**

44 Unicellular organisms substitute phosphorus (P) containing membrane lipids with non-P
45 substitutes when P is scarce, allowing greater growth of populations. Previous research with the
46 model diatom species *Thalassiosira pseudonana* grouped lipids by polar headgroups in their
47 chemical structures. The significance of the research herein is in the description of the individual
48 lipids within the headgroups during P-lipid substitution. This revealed the relationship between
49 lipid headgroups and hints at the underlying biochemical processes. Secondly, P-lipid
50 substitution was contextualised by measurements of total cellular P. This depicted the place of P-
51 lipid substitution in relation to the broader response to P-stress and yields insight into the
52 implications of substitution in the marine environment. Finally, lipids previously unknown in this
53 system were identified. This revealed a new type of non-P substitute lipid, potentially useful as a
54 biomarker to investigate P-limitation in the ocean.

55

56

57

58

59

60

61 Keywords: *Thalassiosira pseudonana*, Phospholipid, Sphingolipid, Diatom, Lipidomics,
62 Phosphorus, Stress, Limitation, Substitution, Biomarker.

63 **Introduction**

64 Diatoms are a diverse group of eukaryotic microalgae responsible for up to 25% of global and 50%
65 of oceanic annual primary production (1). Lipids, hydrophobic or amphipathic biological
66 molecules (2, 3), comprise 25 - 45% of the total dry weight of diatoms (4) representing a major
67 pool of organic carbon. In the equatorial Pacific Ocean, for example, lipids account for 23% of
68 the organic, total planktonic carbon (5).

69 Lipid biosynthesis involves a network of reactions that, through the exchange of polar
70 headgroups and fatty acids, generate a rich variety of lipids (3, 6). Remodelling of a cell's
71 lipidome (the entirety of its cellular lipids) in response to environmental conditions is common in
72 unicellular organisms (7, 8). One such remodelling mechanism utilizes the substitution of
73 membrane glycerophospholipids with non-phosphorus glycerolipid counterparts when an
74 organism is subjected to phosphorus (P) stress or starvation (7–10). This response allows a
75 phytoplankter to reduce its P demands in P-limited environments (9), such as the Sargasso Sea or
76 the eastern Mediterranean Sea. These oligotrophic regions contain very low bioavailable
77 phosphate (PO_4^{3-}) concentrations (typically <10 nmol L^{-1})(9, 11, 12). The reduction in total P
78 demand confers a considerable advantage to growth by allowing for the prioritisation of non-
79 substitutable functions, such as nucleic acid synthesis, over phospholipid biosynthesis (9, 13).

80 The marine diatom *Thalassiosira pseudonana* has been used as a model organism to
81 study the effects of P starvation on lipid remodelling (8, 9). Under phosphorus replete growth
82 conditions (P+) *T. pseudonana* synthesizes glycerophosphatidylcholine (PC),
83 glycerophosphatidylglycerol (PG) and glycerophosphatidylethanolamine (PE) (8, 9). In contrast,
84 when grown under P- conditions it synthesises the nitrogen containing betaine lipid
85 diacylglycerylcarboxyhydroxymethylcholine (DGCC), which is normally undetectable under P+

86 conditions (9). The increase in DGCC is concomitant with a decrease in PC and it is thought that
87 the two physicochemically similar zwitterionic lipids can substitute for each other without loss of
88 membrane function (8, 9, 14). Betaine lipids, including DGCC, are highly abundant in the
89 marine environment (9, 15–18). In addition to the shift between PC and DGCC lipids in P-
90 starved *T. pseudonana*, PG lipids may be exchanged for sulphur-containing
91 sulfoquinovosyldiacylglycerol (SQDG) (8, 9). As such, ratios of the substitute lipid pairs have
92 been considered as biomarkers of P stress in both marine and freshwater environments (9, 19).

93 The biosynthetic pathways underlying these processes are well defined for eukaryotic
94 microalgae in general (20–23) and are coupled with the published genome of *T. pseudonana* (24).
95 The biosynthetic pathway leading to DGCC, is conspicuously unknown, beyond the observed
96 incorporation of radiolabelled methionine (25).

97 PG, and the glyceroglycolipids SQDG, monogalactosyldiacylglycerol (MGDG) and
98 digalactosyldiacylglycerol (DGDG) are enriched in the plastid thylakoid membranes (26).
99 Furthermore, these glyceroglycolipids are biosynthesised within the chloroplast via the
100 intermediate diacylglycerol (DAG). The biosynthesis of cellular membrane lipids including PC
101 and PE is, in contrast, conducted within the endoplasmic reticulum but also proceeds via a DAG
102 intermediate (20–23). As such, the observed total cellular DAG composition may yield insight
103 into lipid metabolism.

104 Lipid substitution kinetics in *T. pseudonana* are rapid, resulting in the exchange of the
105 majority of cellular glycerophospholipids with DGCC and SQDG within 48 h of the initiation of
106 P stress (8). P-starved *T. pseudonana* responds to the resupply of P faster still, restoring the
107 predominance of glycerophospholipids over a 12 - 24 h period (8). P-lipid substitution dynamics
108 have also been examined in other phytoplankton, such as the pennate marine diatom

Phaeodactylum triconutum, resulting primarily in PG to SQDG and PC to diacylglyceryl hydroxymethyltrimethyl-β-alanine (DGTA) substitution, reflecting a contrasting system (27). In addition, a comprehensive recent study in *Emiliania huxleyi* illustrates increased DGCC:PC and SQDG:PG ratios in addition to ultrastructural modifications resulting from P stress (28).

P-lipid substitution in *T. pseudonana* has, therefore, been well characterised in terms of the total lipid within each of the major polar headgroup classes. However, important unknowns remain:

The dynamics of the individual lipid chemotypes, differentiated by the fatty acids they bear, subject to P stress remain unknown. Revealing these dynamics has the potential to yield insight into mechanisms of P-lipid substitution such as the synthesis of DGCC. Secondly, the effects of P-lipid substitution upon particulate organic P (POP) content per cell have not been reported. Consequently, the relationship between the responses associated with lipidic and extra-lipidic POP remains unknown. Moreover, previous work has not provided a comprehensive discussion of the relative contributions of two potential underlying mechanisms for P-lipid substitution, i.e. active break down of glycerophospholipids and replacement with non-P alternatives vs a simple switch in biosynthesis to the production of non-P lipids (29). Finally, the behaviour of minor lipid species, outside of the predominant headgroup classes, has yet to be studied. The cellular response to P stress is complex and powerful (30). It is expected therefore, that lipids other than those most common and abundant groups studied to date, are also affected. These minor species may display novel substitute or biomarker behaviour.

Presented herein, the findings of a mass spectrometry based lipidomics study, using both targeted and untargeted methodologies to characterise the lipidic response to P stress in cultures of *T. pseudonana.* These methods, coupled with culture growth monitoring, dissolved, and

132 particulate nutrient concentrations, yielded novel insight into the kinetics of P-lipid substitution,
133 in relation to the broader cell response to P stress. In addition, the data on individual lipid species
134 indicated the declining PC lipid pool became relatively enriched in unsaturated lipid species.
135 Finally, untargeted lipidomic screening revealed diglycosylceramide sphingolipids that displayed
136 lipid substitute/biomarker behaviour in the P stressed cultures. These findings offer a deeper
137 understanding of the dynamics of P-lipid substitution in marine phytoplankton, a fundamental
138 mechanism for growth in P scarce seas, and its cellular implications.

139

140

141 **Results**

142 **Phospholipid Substitution and Particulate Organic Phosphorus Dynamics**

143

144 *Figure 1*

145

146 Statistical significance of comparisons is indicated in the following text as *p<0.05 **p<0.005
147 by two-tailed, paired equal-variance T-test.

148 During exponential growth of the cultures (Figure 1A) between 0 and 72 h, the P+
149 cultures grew at a rate of 0.029 ± 0.0013 h^{-1} (23.76 ± 1.08 h doubling time). Exponential growth
150 during the same period in the P- cultures was marginally slower at 0.026 ± 0.0016* h^{-1} (27.09 ±
151 1.78 h doubling time). Both the P+ and P- cultures appeared to be transitioning into stationary
152 phase at 96 h with maximum populations of 1.08 x 10^6 ± 4.11 x 10^4 cells mL^{-1} and 1.14 x 10^6 ±
153 7.35 x 10^4 cells mL^{-1} respectively. Culture viability was high throughout at >90 %, in both P+
154 and P- cultures, with the exception of the P- cultures at 48 h (87.95 ± 1.78 %) (Supplementary
155 Figure 1E), the cultures were therefore considered to be healthy and not subject to stresses other
156 than P up to 72 h.

157 Dissolved phosphate ([PO_4^{3-}], Supplementary Figure 1D) in the phosphorus replete (P+)
158 control cultures was in excess (>10 µmol L^{-1}) throughout the 96 h course of the experiment.
159 [PO_4^{3-}] in the phosphorus stressed (P-) cultures at 0 h was 0.80 ± 0.00 µmol L^{-1}, dropping to 0.20
160 ± 0.00 µmol L^{-1} after 6 h. This indicates a minor carryover of P from the P replete seed cultures
161 to the P- culture treatment, which was depleted around 6-12 h thus subjecting the P- cultures to P

stress. Dissolved nitrate ([NO_3^-]) and silicate (orthosilicate ions [SiO_4^{4-}]) concentrations remained in excess throughout, in both P+ and P- cultures (Supplementary Figure 1A, B), with the exception of the P+ cultures after 72 h in which [SiO_4^{4-}] was depleted. The cultures were, therefore, not subject to confounding macronutrient stress, with the possible exception of the P+ 96 h samples. Taken together, the growth and nutrient data suggest the 96 h P+ samples were entering an Si limited stationary growth phase. These data will therefore, not be considered as a basis for drawing conclusions about P stress hereafter, but the data are included for context.

Particulate organic phosphorus (POP) quantity per cell (Figure 1B) fell with the progression of P stress through time, in the P- cultures. Initial P- POP was 1.94 ± 0.26 fmol $cell^{-1}$ and dropped consistently over 96h to a minimum of 0.25 ± 0.028 fmol $cell^{-1}$ at 96 h, equivalent to a 0.11 ± 0.03** fold reduction relative to the concurrent P+ control samples. The determined POP quantities per cell for the P+ cultures of between 1.79 ± 0.07 and 2.84 ± 0.22 fmol $cell^{-1}$ are approximately in line with previous observations for *T. pseudonana* of 2.8 – 6.2 fmol $cell^{-1}$ (31).

Total phospholipid (Figure 1C) represents the sum of the predominant phospholipid classes: glycerophosphatidylcholine (PC), glycerophosphatidylglycerol (PG), and glycerolphosphatidylethanolamine (PE). The individual dynamics of these lipid classes are shown in Supplementary Figure 2. Total P-lipid showed an initial increase in both P+ and P- cultures between 0 and 6 h, from 0.73 ± 0.08 to 1.25 ± 0.05 fmol $cell^{-1}$ in the case of the P- cultures and declined rapidly thereafter to a minimum of 0.17 ± 0.02 fmol $cell^{-1}$ at 96 h, equivalent to a 0.08 ± 0.01 fold reduction relative to the P+ control cultures.

The betaine lipid Diacylglycerylcarboxyhydroxymethylcholine (DGCC, Figure 1D), was absent from the P+ cultures throughout and the P- cultures before 12 h. Concomitant with the

184 decline in P-Lipid, DGCC quantities increased through time in the P- cultures following 12 h to
185 reach a maximum of 0.85 ± 0.075 fmol cell^{-1} at 48 h and 0.67 ± 0.036 fmol cell^{-1} at 96 h.

186 The sulfolipid sulfoquinovosyldiacylglycerol (SQDG, Supplementary Figure 2E), was
187 1.31 ± 0.14* fold greater in quantity in the P- cultures than the P+ control at 6 h. SQDG
188 quantities were then statistically similar in P+ and P- between 12 and 72 h, followed by a 0.71 ±
189 0.045** fold reduction in the P- cultures, relative to P+ at 96 h. SQDG therefore, did not vary
190 significantly in a consistent manner in response to P stress and did not appear to act as a
191 substitute lipid for PG in this case, as found in other systems (9).

192 Diacylglycerol (DAG, Supplementary Figure 2D) quantity per cell did not vary
193 significantly between P+ and P- cultures, with the exception of a 0.58 ± 0.10* fold reduction in
194 the P- cultures at 96 h. To our knowledge DAG has not been previously characterised in P
195 stressed *T. pseudonana* cultures and did not vary significantly and consistently in response to P
196 stress.

197 Neutral storage lipids were not quantified in this study which was focused on polar and
198 phosphorus containing membrane lipids. However, for context, it is known that diatoms
199 biosynthesize large reserves of (non-P containing) triacylglycerol (TAG) storage lipids subject to
200 P stress (32). This leads to an overall increase in total glycerolipids in the similarly sized pennate
201 diatom *P. tricornutum*, subject to P stress (27).

202

203 **P-Lipids vs. Non-Lipidic Particulate Organic Phosphorus**

204 The difference between total POP and total P-lipid (Figure 1E) was used to investigate the
205 dynamics of the non-lipid associated (Non-Lipidic) POP within the overarching P stress scenario.

206 In the P- cultures, the non-lipidic POP declined rapidly from 1.21 ± 0.27 to 0.083 ± 0.17 fmol
207 cell^{-1} over the course of the first 12 hours, remaining approximately constant thereafter. Non-
208 lipid POP in the P+ cultures, in comparison, remained statistically constant during the same time
209 interval, decreasing over the course of 72 h from 1.19 ± 0.38 to 0.19 ± 0.12 fmol cell^{-1}.

210

211 **Degradation/Interconversion vs. Substitution by De novo Synthesis**

212 The rates of change of P-lipid per cell and cell concentration were calculated (Figure 1F) to
213 enable the distinction between a per cell 'dilution' whereby the original P-lipid was divided up
214 amongst successive generations of progeny cells versus the chemical degradation and breakdown
215 of the original P-lipid. The observations were made relative to the 12 h samples due to the
216 initiation of P-lipid substitution at that time as evidenced by the depletion of dissolved P
217 (Supplementary Figure 1D) and the commencement of DGCC synthesis (Figure 1D). The loss
218 rate of P-lipid per cell of -0.031 ± 0.0015 h^{-1} was 32.29 ± 10.91** % faster than the dilution rate
219 by culture growth of -0.023 ± 0.0015 h^{-1} (Figure 1F). The additional loss at greater than the rate
220 of cell dilution is indicative of degradative breakdown.

221 In addition, the difference in total phospholipid per unit volume culture, between time (t)
222 and 12 h in the P- cultures ($\Delta PL_{t\text{-}12h}$) was also used to assess the total quantity of lipid per culture,
223 regardless of per cell quantities (Supplementary Figure 2F). At 48 and 72 h in the P- cultures,
224 $\Delta PL_{t\text{-}12h}$ was -42.27 ± 18.19* pmol mL^{-1} and -80.47 ± 20.03** pmol mL^{-1} respectively, indicating
225 a net degradation of the total phospholipids at these times. The P liberated from P-lipids between
226 12 and 72 h was 7.66 x 10^7 ± 1.95 x 10^7 atoms per daughter cell grown during that time,
227 equivalent to 1.06 ± 0.55 diploid genomes per cell (8, 33). Therefore, the P released from P-lipid

228 breakdown appeared sufficient to cover DNA biosynthesis requirements for growth during this
229 time interval.

230 The maximum degradative decrease in $\Delta PL_{t\text{-}12h}$ at 72 h (Supplementary Figure 2F)
231 corresponded to a loss of 34.10 ± 8.75 % of the maximum total phospholipid observed at 12 h in
232 the P- cultures. This value is consistent with the P-lipid degradative loss rate calculated
233 previously (32.29 ± 10.91** % faster than the dilution rate by culture growth) over the same time
234 interval. In comparison, the change in total DGCC ($DGCC_{t\text{-}12h}$) increased rapidly through time
235 reaching +464.90 ± 50.05 pmol mL^{-1} at 72 h. Taken together, the molar degradative decrease in
236 $PL_{t\text{-}12h}$ was equivalent to 17.31 ± 4.69 % of the increase in DGCC.

Fatty Acid Level Response to Phosphorus Stress

Figure 2

Variation in individual lipid species quantity, between P+ and P- cultures at 72 h is shown in Figure 2. All PC species (Figure 2A) showed a dramatic decrease in quantity per cell in the P- cultures, by comparison to the P+ control cultures. Some variation in the magnitude of this decrease was evident from the data: PC(18:4/16:0) and PC(20:5/18:4) showed the largest fold decreases of 0.018 ± 0.0035** and 0.023 ± 0.037** fold respectively. PC(16:1/16:0), PC(20:5/16:1), PC(20:5/16:0) and PC(38:6) showed highly significant, intermediate fold decreases between 0.053 ± 0.011 and 0.15 ± 0.043. In contrast, highly unsaturated PC(22:6/20:5) and PC(20:5/20:5) species displayed the smallest fold decreases of 0.28 ± 0.054** and 0.30 ± 0.052** fold respectively.

Betaine lipid DGCC species (Figure 2B) occurred only in the P- cultures and were below detection in the P+ control cultures. At 72 h, the five most abundant DGCC species in the P- cultures were DGCC(20:5/16:0), DGCC(22:6/20:5), DGCC(20:5/20:5), DGCC(38:6) and DGCC(20:5/16:1), with quantities of 84.28 ± 14.14, 60.08 ± 9.39, 56.56 ± 11.87, 50.56 ± 7.40 and 33.05 ± 6.16 amol cell^{-1} respectively.

Glycerophospholipid PE species (Figure 2C) decreased in the P- cultures relative to the P+ control cultures. The predominate PE lipid species PE(22:6/20:5), PE(20:5/20:5) and PE(20:5/16:1) decreased by 0.19 ± 0.065**, 0.18 ± 0.060* and 0.07 ± 0.028** fold respectively under P stress.

259 The glycerophospholipid PG (Figure 2D) behaved in line with PC and generally
260 showed a decrease in quantity per cell for its molecular species in the P- cultures, relative to
261 the P+ control cultures. The predominant chemotypes, PG(16:1/16:0)**; PG(20:5/16:0)*;
262 PG(20:5/16:1)**; PG(16:1/14:0)**; and PG(32:2)** all exhibited fold decreases of between
263 0.062 ± 0.027 and 0.11 ± 0.048 subject to P stress.

264 Bivariate analyses (Supplementary Figure 3) were used to compare the relative
265 abundance of individual lipid species within pairs of lipid classes, in order to provide an
266 indication of similarity in their fatty acid distributions. Overall, when considering the
267 distributional similarity between all the measured lipid classes in both treatments, at all time
268 points between 12 and 72 h, two primary clusters were observed: The first cluster was
269 comprised of PC, its substitute DGCC, and PE and bore similar fatty acid distributions with
270 an average pairwise correlation coefficient (r) of 0.68 ± 0.25. A second cluster, of PG, DAG,
271 MGDG and DGDG fatty acid distributions was highly cross correlated with r = 0.87 ± 0.10.
272 In addition, these two clusters were highly distinct from each other, with r = 0.074 ± 0.18.
273 Interestingly, DGCC was moderately correlated with DAG at 12 h, with r = 0.53 ± 0.023 and
274 weak to no relationship thereafter. DGCC abundance at 12 h was, however, negligible
275 compared to 24 h and later.

276 The absolute quantities of degradative loss of PC individual lipid species were weakly
277 correlated with DGCC gains (Supplementary Figure 4D, E and F) for time intervals of t48-
278 t24 h and t72-48 h in the P- cultures, with coefficients of determination between R^2 = 0.3**
279 and 0.17* respectively. The linear regression coefficients were consistent with 18 and 20%
280 respectively of the DGCC synthesised at these time intervals originating as recycled
281 diglyceride moieties from degraded PC. This estimate is further consistent with the
282 cumulative degradation of PC between 12 and 72 h, presented previously, of 17.31 ± 4.69 %
283 of the increase in DGCC at the total class level (Supplementary Figure 2F).

284

285 **Fatty Acid Level Variability during P-replete Growth**

286

287 *Figure 3*

288

289 In order to study the temporal dynamics of P-lipids in the context of P stress at the individual
290 lipid species level, the top 5 most abundant PC lipids, as the predominant components of the
291 total P-lipid pool, were analysed in isolation. Firstly, the underlying dynamics of the P+
292 control cultures were considered (Figure 3A). The top five PC molecular species, as ranked
293 by their maximum quantity per cell, appeared to conform to one of two behaviours. The
294 highly unsaturated PC(20:5/20:5) and PC(22:6/20:5) chemotypes displayed a sharp increase
295 between 0 and 12-24 h with the initiation of exponential growth, followed by an equally
296 sharp decline in abundance to 72 h. PC(22:6/20:5), for example, rose from 18.11 ± 4.39 at 0 h
297 to 168.57 ± 9.83** at 24 h, before dropping back to 39.67 ± 7.28** amol $cell^{-1}$ by 72 h. In
298 contrast, moderately unsaturated species PC(18:4/16:0), PC(20:5/18:1), and PC(20:5/18:4)
299 displayed a consistently increasing trend with the progression of time in the P+ control
300 cultures. PC(20:5/18:4), for example, increased from 36.21 ± 7.44 at 0 h to 159.26 ± 39.81*
301 amol $cell^{-1}$ at 96 h.

302 To decouple the P stress driven dynamics from the growth driven dynamics, the
303 change in PC lipid quantity through time, relative to the initiation of P stress in the P- cultures
304 at 12 hours was determined (Figure 3B). Overall, the top 5 PC lipids all exhibited a
305 continuous decreasing trend in quantity between 12 and 96 h subject to P stress. The
306 magnitude of change was variable between different lipid species, with PC(20:5/18:4) and

307 PC(20:5/18:1) decreasing by 0.52 ± 0.081** and 0.16 ± 0.025** fold respectively. The
308 response of PC(22:6/20:5) was an exception, showing an initial 1.46 ± 0.11 fold increase
309 between 12 and 24 h, followed by a large 0.33 ± 0.073** fold decrease (relative to 12 h). The
310 least unsaturated of the major PC lipids, PC(18:4/16:0) showed the most rapid initial decrease
311 between 12 and 24 h dropping by 0.64 ± 0.070 fold.

312 The variability in the response of these PC lipids to P stress was reflected in the
313 changing average unsaturation of the PC lipid pool through time (Figure 3C). Average PC
314 unsaturation (the total number of fatty acid double bonds) in both P+ control and P- cultures
315 displayed a sharp increase in average PC lipid unsaturation between 0 and 12 h, from 5.73 ±
316 0.098 to 7.53 ± 0.24 in the P+ case. After 12 h, the results diverged between the treatments,
317 concomitant with the initiation of P stress. The P+ cultures then displayed a decrease in
318 average PC unsaturation to 5.63 ± 0.077 at 72 h, remaining constant thereafter. The P-
319 cultures, in contrast, continued increasing to a maximum of 7.95 ± 0.14 at 24 h, followed by a
320 decline until 96 h to 6.37 ± 0.25, but remained more highly unsaturated than the P+ control
321 cultures throughout.

322 These observations co-occur with the P- cultures experiencing decreasing per cell
323 quantities of P-lipids and a minor degree of degradative breakdown as described herein
324 (Figure 1C). Therefore, the initial shift to higher unsaturation in the P- cultures indicates that
325 P stress causes either a preferential degradation of less saturated PC lipids or the continued
326 synthesis during early P stress of low quantities of highly unsaturated PC lipids between 12
327 and 24 h (both mechanisms appear supported by Figure 3B). At later time points, this ceases
328 and the average PC unsaturation begins to decrease and trend toward (but not achieve)
329 convergence with the P+ control values. Overall, a more highly unsaturated PC lipid pool
330 occurs subject to P stress (Figure 3C).

331

332 **Untargeted Lipidomic Screening**

333

334 *Figure 4*

335

336 Lipid species were ranked according to their normalised abundance, in descending order from
337 the most strongly increased under P stress (Figure 4B). The betaine lipid
338 diacylglycerylcarboxyhydroxymethylcholine (DGCC) dominated the positive ion results
339 comprising 14 of the top 15 ions. DGCC species containing eicosapentaenoic (20:5),
340 docosahexaenoic (22:6) and palmitic (16:0) fatty acids, displayed the greatest differential
341 increases and were hence the highest ranked.

342 Most remarkably, a 1014.7112 Da species, corresponding to a diglycosylceramide
343 with a dihydroxy(18:3) long chain base and a 24:0 fatty amide ($(Gly)_2Cer(d18:3/24:0)$) with a
344 formic acid adduct, displayed an absence-presence response to P stress. The chemical
345 structure, and its determination by MS2 fragmentation in both negative and positive ion mode,
346 is displayed in Supplementary Figure 5.

347

348 *Figure 5*

349

350 Several lipids closely related to $(Gly)_2Cer(d18:3/24:0)$ were subsequently observed using
351 more sensitive semi targeted analyses in positive ion mode (Figure 5). Of those,
352 $(Gly)_2Cer(d18:3/24:0)$ itself responded the strongest to P stress with a 10.43 ± 3.12** fold
353 increase between the P- and P+ cultures. Each of the glycosphingolipids displayed a

statistically significant increase subject to P stress, albeit of varying magnitudes. $(Gly)_2$Cer(d18:3/24:1), $(Gly)_2$Cer(d18:2/24:0) and $(Gly)_2$Cer(d18:1/24:0) increased by 6.67 ± 1.81**, 4.89 ± 1.76** and 2.03 ± 0.36** fold respectively, between the P- and P+ cultures. The ceramide equivalent lipid Cer(d18:3/24:0), without the diglycosyl headgroup, was also detected. In contrast, its differential abundance between P- and P+ cultures showed no significant change.

Discussion

Phospholipid Substitution and Particulate Organic Phosphorus Dynamics

We find that the dynamics of P-lipid substitution in *T. pseudonana* follow primarily a cessation of P-lipid net biosynthesis with a minor degree of P-lipid net breakdown (Figure 1). The P liberated by degradative breakdown of P-lipids was enough to synthesise approximately one diploid genome per cell during the same time period of P-stressed growth, one fourth of previous estimates (8). The majority of the original cellular P-lipids were retained and diluted in per cell terms with the progression of culture growth by cell division, consistent with the observed decrease in per cell POP. No appreciable growth limitation occurred on these timescales, reflecting the great capacity of this organism, not least with respect to its lipidomic flexibility, to adapt to low P environments (30).

Non-lipidic P per cell was observed to decrease to near zero after 12 h and warrants discussion, given the expected obligate cellular P requirements for essential genomic and other biomolecules. The minima in non-lipidic P of 0.076 ± 0.058 fmol cell^{-1} at 24 h is just barely sufficient to account for the estimated P associated with DNA per cell (63.74 ± 48.64% estimated from (33)), when the upper standard deviation limit is included. Therefore, it is possible that the measured total POP quantities represent a slight underestimate. This is supported by the measured P+ POP per cell quantities, which are shown in the results section to be consistent with the lower limits of literature values. Nonetheless, the relative shift from the initial state toward a minimum value after 12 h, remains a robust observation appropriate for further discussion.

Non-lipidic POP declined toward its minimum by 12 h, prior to the initiation of the P-lipid response. The temporal delay in the lipid remodelling response to P stress may be attributable to the prior utilisation of P from other intracellular pools. Polyphosphates (polyP)

384 could be one such pool (34), however these observations conflict with recent environmental
385 observations which suggest polyP enrichment of phytoplankton in P-limited waters (35). To
386 our knowledge, polyP has not been quantified in *T. pseudonana* to date, so this contradiction
387 cannot be reconciled at this point.

388 The majority of the original lipid bound P remained as such and did not appear to be
389 made available for other cellular processes such as nucleic acid synthesis (8, 27). This does
390 not diminish the ability of the organism to grow subject to reduced P availability by utilising
391 non-phosphorus containing lipids rather than phospholipids. The distinction has subtle
392 conceivable ecological implications. Heterotrophic bacteria that consume lipids efficiently
393 (36), for example, may benefit from access to lipidic P content in oligotrophic waters.
394 Additionally, assuming that the use of non-phosphorus containing lipids rather than
395 phospholipids has little physiological influence on cell growth, the phospholipid content of P
396 replete cells arguably represents an enigma if this P pool is not strongly re-purposed on
397 development of P-stress.

398 The stable abundance of SQDG throughout could be interpreted as an adaptation to
399 economize on P requirements in the oceanic environment in which P is regularly scarce. The
400 substitute lipid pair, PG and SQDG, share at least a partial functional similarity/redundancy
401 in their role in the thylakoid membranes (10, 26). However, the efficiency of photosystem II
402 is demonstrably compromised in SQDG deficient algal mutants (37), suggesting SQDG has
403 an essential functional role and is not only a non-P substitute for PG.

404 Overall, this deeper understanding of a powerful phytoplankton adaptation to P-stress
405 gives greater context to the resulting dramatic shifts upon elemental ratios and phytoplankton
406 growth dynamics, with subsequent implications to both trophic transfer and export flux.

407

Fatty Acid Level Response to Phosphorus Stress

PC individual lipid quantity per cell was highly dynamic in the P+ control cultures with the progression of the time (Figure 3A). The most highly unsaturated PC lipids increased markedly in early exponential growth before declining back to initial levels later as the cultures progressed toward stationary growth phase. More saturated major PC lipids displayed a progressively increasing quantity per cell through time. These observations are in agreement with previous reports on the relationship between unsaturation of eukaryotic phytoplankton glycerolipids and growth phase (38). The change in lipid unsaturation state arises from the partitioning between polar and neutral storage lipid biosynthesis, which proceed via distinct elongation and desaturation pathways (38). When growing rapidly, polyunsaturated fatty acids characteristic of the structural polar lipids are biosynthesised. However, during the transition to stationary growth, more saturated fatty acids are synthesised for incorporation into TAG storage lipids. This is reflected in part in the polar glycerolipids due to a degree of crosstalk (38).

The discussed variation in membrane glycerolipid composition should have subsequent functional implications upon membrane biophysics and structure, unless homeostatically compensated in some other manner (39). The complexity and degree of the temporal changes in the individual lipid species composition, within the P+ control cultures, highlight the lipidomic plasticity of *T. pseudonana* and its highly dynamic nature, both often poorly accounted for in biomarker studies. This behaviour contributes to a lack of diagnostic power for chemotaxonomic distinction of phytoplankton that has been reported elsewhere with respect to fatty acids (40) and intact polar lipids (18).

In the P- cultures, we observe a preferential degradation of more saturated PC lipid species and/or a continuing synthesis of highly unsaturated PC lipids, leading to a more

highly unsaturated, less abundant PC lipid pool (comprising the majority of the P-lipids) under P stress (Figure 3B, C). It could be speculated that this increase in unsaturation represents a homeostatic control on membrane fluidity (as in (39)) in light of the increasing substitution of P-lipids by DGCC, which may result in differing biophysical characteristics.

DGCC, which increased in cellular abundance with the progression of P stress, was correlated in chemical composition with PC (Figure 2 and Supplementary Figure 3). This similarity in composition is consistent with the role of DGCC as a substitute lipid for PC in *T. pseudonana* (8, 9), and the observation provides further evidence for the substitutive link between the two.

The molar quantity of P-lipid breakdown accounted for a minor proportion of the biosynthesised DGCC at the total class level. In addition, the degradative loss of individual PC lipid species was weakly correlated with the synthesis of their DGCC counterparts (Supplementary Figure 4). These data are consistent with, but not definitive evidence of, the recycling of diglyceride moieties from phospholipid breakdown for incorporation into newly biosynthesised DGCC. This observation must be further confirmed by an isotopic labelling experiment to unambiguously trace the transformation.

DAG is a known direct precursor in eukaryotes to glycerophospholipids (PC, PE)(20). Under P- conditions, an uncoupling of the DAG composition with the glycerophospholipids could be expected if they are not being synthesised. However, DAG composition did not vary between P+ and P- conditions as previously discussed. Therefore, we expect the composition of lipid species in the DAG to reflect that of PC, the most abundant of its biosynthetic products, under P+ conditions but that was not the case. Furthermore, no consistent correlation was observed between DGCC and DAG. As the precursor to PC biosynthesis (20) and a substructure in common to both PC and DGCC, DAG is a potential intermediate in the

456 synthesis of DGCC. This could occur via de novo synthesis or represent a recycling of any
457 diglyceride from PC breakdown via phospholipase C. Again, our observations do not support
458 these hypotheses. PC is synthesised from DAG under P+ conditions, yet we cannot observe
459 this via the correlation of its individual lipid species. Based on these results, a role of DAG in
460 the biosynthesis of DGCC cannot be ruled out. Unfortunately, comparison of the various
461 polar lipid distributions did not yield significant insight into the as yet unknown biosynthetic
462 pathway leading to DGCC. To our knowledge, nothing appears known other than the
463 reported incorporation of 14C labelled methionine into its head group in labelling
464 experiments (25, 41). This remains a very conspicuous gap in our understanding of a lipid
465 class that forms a major component of the planktonic lipid pool (42).

466 Thus, it appears that the observed DAG is utilised primarily by
467 monogalactosyldiacylglycerol synthase as a biosynthetic precursor to MGDG and DGDG (21,
468 24). These observations lead to the formation of the hypothesis that there are two (or more)
469 separate pools of DAG. Firstly, the larger and/or slower turned over DAG pool indicative of
470 MGDG/DGDG synthesis, observed by characterisation of the total lipid extract and localised
471 within the chloroplast. Secondly, the smaller and/or more rapidly turned over DAG pool
472 indicative of PC/PE synthesis that is conspicuously not observed. Further investigation of
473 DAG lipid dynamics within isolated subcellular locales may yield further insight into the link
474 between DAG and the biosynthesis of PC and DGCC.

475

476 **Untargeted Lipidomic Screening**

477 Untargeted lipidomic screening revealed $(Gly)_2Cer(d18:4/24:0)$ which was approximately 10
478 fold more abundant in the P- than the P+ cultures. This discovery led to the identification of a
479 series of related molecules varying subtly in the degrees of unsaturation of the long chain

480 base or the fatty acid amide (Figure 5). All of the diglycosylceramide species increased under
481 P stress, varying in magnitude of change between approximately 2 and 10 fold. A
482 Cer(d18:3/24:0) species was also identified and demonstrated contrasting behaviour. This
483 putative precursor did not vary in cellular abundance subject to P stress. Chemically identical
484 and related lipids have been previously reported in another marine diatom, *Skeletonema*
485 *costatum* (43) and genes encoding sphingolipid biochemistry are also annotated in the
486 genome of *T. pseudonana* (24). This lends further credence to our identification and
487 highlights these molecules as an area of interest for future research into diatom lipid
488 biochemistry. Glycosylceramides have been ascribed to several physiological functions
489 including membrane stability, membrane permeability and pathogenesis (44). In this context,
490 it appears that they may be acting as non-phosphorus substitute lipids, akin to DGCC (8–10),
491 for another phosphorus containing lipid and this drives their differential increase under P
492 stress.

493 Chemically closely related glycosphingolipids have been identified in virally infected
494 *Emiliania huxleyi* and applied as biomarkers for viral infection in the marine environment
495 (45–48). In the same manner, we propose the diglycosylceramides that increase in cellular
496 abundance subject to P stress, as candidate biomarkers for the P stress of marine diatoms in
497 the environment. As such, the abundance of these potentially diagnostic biomarkers could be
498 quantified in diatoms collected from the environment of interest. This data could yield
499 additional insight into the level of P stress experienced by the phytoplankton directly, which
500 would be complimentary information to the more routine measurement of dissolved or
501 particulate P concentrations in the medium. Targeted quantification of these lipids would be
502 readily achievable using commercially available lactosyl-ceramide standards as in (43). Such
503 a lipid biomarker could be useful to follow P related biogeochemical processes in the
504 environment, pending further validation. More broadly, the discovery of this sphingolipid

505 behaviour, taken together with the *E. huxleyi* host/virus system strongly supports
506 phytoplankton sphingolipid biochemistry as an important avenue for future research.

Conclusions

We have presented herein the comprehensive lipid analysis of phospholipid substitution induced by P stress in the model marine diatom *T. pseudonana* at the level of individual lipid species, those varying in fatty acid composition, and in tandem with quantification of cellular particulate organic phosphorus (POP). These data indicate depletion of a non-lipidic POP fraction, prior to the lipid response. This was followed immediately thereafter by de-novo biosynthesis of the substitute lipid DGCC. The majority of the original P-lipid remained intact and was diluted amongst progeny cells but P equivalent to approximately one diploid genome per daughter cell was liberated by degradative breakdown of P-lipids. The distinction between P associated ultimately with lipids as opposed to genomic material may have implications upon subsequent trophic transfer and export flux.

At the individual lipid level, all major P-lipids reduced in cellular quantity but in a non-uniform manner. P stress resulted in an increased average degree of unsaturation within the declining PC lipid pool, which represented the predominant P-lipids. These observations indicate a preferential degradation of more saturated PCs and/or a continuing synthesis of highly unsaturated PC lipids, perhaps in order to regulate membrane fluidity in the context of the major change in membrane composition through substitution. Further, the data were tentatively consistent with the recycling of diglyceride substructures from P-lipid degradation into newly synthesised DGCC.

DAG fatty acyl composition primarily reflected that of the chloroplast associated glyceroglycolipids and did not yield insight into the biosynthetic pathway of the substitute lipid DGCC. This pathway remains a significant gap in our understanding of a biochemical highly abundant in the marine environment.

Finally, untargeted lipidomic screening revealed a group of diglycosylceramide lipids which increased subject to P stress up to 10 fold and constitute non-phosphorus substitute lipids and candidate biomarkers for P stress. Taken together, these findings contribute a new level of understanding of P-lipid substitution in marine phytoplankton, a powerful and widespread adaptation to low P environments with important consequences upon macronutrient biogeochemistry and oligotrophic primary production.

Experimental Procedures

Culturing

Axenic *T. pseudonana* (1085/12 also designated CCMP1335/3H) was obtained from the Culture Collection of Algae and Protozoa, Scottish Association for Marine Science, U.K. Culture manipulations were performed under sterile, laminar flow environment.

F/2+Si growth media (49), based on artificial seawater was prepared (50) from analytical or biological grade components (Fisher Scientific). Seed culture (175 mL) was grown to mid-log phase concentration of 1.13 x 10^6 cells mL^{-1} over 4 days incubation at 18°C; 12:12h light/dark cycle; 123 µmol quanta m^{-2} s^{-1} illumination; 70 rpm gentle orbital agitation.

The seed culture was split (2 x 79.6 mL) and cells isolated from the media by filtration (Millipore Steritop, 0.22 µm pore size). Cells were washed on the filter with 50 mL of P+/P- media, depending on treatment, then resuspended and split to form 3 x 300 mL for each P+ and P-. These experimental cultures were incubated as above and sampled after 0; 6; 12; 24; 48; 72 and 96 hours for size distribution/cell count; viability; dissolved/particulate macronutrients and lipid extracts.

An aliquot (950 µL) of culture was mixed with freshly prepared paraformaldehyde solution (170 µL, 34% w/v, dH_2O) and stored at 4°C for <24 h before analysis. Cell size distributions were generated with a Beckmann Coulter Multisizer 3 Coulter Counter. A 70 µm aperture and 3% NaCl electrolyte were used and the samples diluted to ensure <10 % aperture coincidence concentration. The Coulter Counter was calibrated with 5.023 µm polystyrene latex standard beads prior to use (Beckmann Coulter via Meritics Ltd., Dun-stable, U.K.). Size distributions were used to generate cell concentration values, between the limits of 3 and 9 µm particle diameter.

559 Experimental culture (50µL) was incubated with SYTOX-Green dye (Invitrogen Life
560 Technologies, Paisley, U.K.) at a concentration of 0.5µM for 5 minutes in the dark. 18 µL of
561 this solution was then imaged with a Cellometer Vision Duo (Nexcelcom Bioscience via.
562 Peqlab, Sarisbury Green, U.K; X100-F101 Optics; SD100 Slides). All cells were counted
563 manually under brightfield mode and stained, non-viable cells under fluorescence mode
564 (470/535nm excitation/emission).

565

566 **Nutrient Quantification**

567 Experimental culture (10 mL) was syringe filtered over pre-combusted (450°C, 12h) GF/F
568 filters. The filtrate was stored at -20 °C. Filters were dried at 60°C for 24 h and stored in a
569 desiccator. Particulate phosphorus was determined following an oxidation procedure as
570 described in reference (51), samples were centrifuged (1000 x G, 10 mins, 18 °C) before
571 sampling to remove particulates. Nutrient samples were diluted: 1/60 (dissolved nutrients
572 (filtrate)) and 3/20 (oxidised particulate nutrients) in milliQ dH_2O and characterised by
573 segmented flow autoanalysis on an AutoAnalyzer 3 (Seal Analytical, Fareham, U.K.) for
574 phosphorus, nitrate/nitrite and silicon. POP quantities were corrected for carryover of
575 inorganic phosphate from the growth media based upon the difference between the P+ and P-
576 POP measured at 0 hours, normalised to the $[PO_4]^{3-}$ concentration in the P+ growth media for
577 a given sample (as measured by the dissolved phosphate (DIP) assay):

578 $$((POP^{P+}{}_{t0})-(POP^{P-}{}_{t0}))*((DIP^{P+}{}_{t})/(DIP^{P+}{}_{t0}))$$

579

580 **Lipid Extraction**

581 Lipid samples (20 mL) from the experimental cultures were isolated by syringe filtration as
582 above. The filtrate was discarded and the filters stored at -78 °C until extraction. Total lipid
583 extracts were prepared using a Bligh-Dyer extraction procedure (52) as modified by (53).
584 Solvents were LC-MS grade (Fisher Scientific). Lipid internal standards were added at
585 quantities adjusted per sample to maintain constant standard:cell equivalents ratios as follows:
586 PC(12:0/12:0)(56.2 amol cell-1); PG(12:0/12:0)(77.0 amol cell-1); PE(12:0/12:0)(47.6 amol
587 $cell^{-1}$); DAG(20:4/18:0)(99.7 amol $cell^{-1}$) and SQDG (mixed extract, predominantly
588 34:3)(1.27 fmol $cell^{-1}$). Phospholipid/DAG standards were acquired from Avanti Polar Lipids
589 (Alabaster, U.S.A.), SQDG spinach leaf extract was provided by Lipid Products (Surrey,
590 U.K.).

591 A variable volume of this phase was isolated per sample ensuring a constant quantity
592 of lipid cell equivalents/standard quantity was infused into the mass spectrometer during
593 analysis (hence accounting for ion suppression and enabling external standard quantification
594 of DGCC). The optimal quantity for analysis under instrument/conditions below was found to
595 be 0.8 x 10^6 cells (+standards as described). This fraction was dried under N_2 and stored at -
596 20°C until analysis.

597

598 **Direct Infusion ESI-MS/MS Quantitative Analysis**

599 Mass Spectrometric analysis was performed on a Waters Micromass Quattro Ultima triple
600 quadrupole instrument. Dried samples were dissolved in 250µL 66% methanol, 30%
601 dichloromethane, 4% ammonium acetate (300 mM in H_2O). The sample solution was directly
602 infused into the instrument at 6µL min^{-1} and analysed by MS/MS analysis of each lipid class
603 (53). In addition, a neutral loss scan of 35 Da, between 350-750 Da at a collision energy of 15
604 eV, was used for the detection of ammoniated DAG molecular ions.

605 Spectra were processed by despiking, baseline subtraction, isotopic correction and
606 assignment by a visual basic macro (54). The spectrum of the SQDG standard in isolation
607 was taken in triplicate and used to perform a subtraction for overlapping standard derived
608 peaks (due to the natural extract nature of the SQDG standard) based on the dominant peak at
609 834 Da (SQDG34:3, not detectable in *T. pseudonana* under P+/P- conditions). DGCC extract
610 (purified by preparative HPLC from *T. pseudonana* under P starvation) was provided by
611 Benjamin A. S. Van Mooy (Woods Hole Oceanographic Institute, U.S.A.). External standard
612 calibrations were generated from addition of DGCC extract (0.094; 0.19; 0.38; 0.75; 1.5 nmol)
613 to P-replete grown (hence no intrinsic DGCC) *T. pseudonana* total lipid extracts prepared at
614 optimal, constant cellular lipid/standard concentration as previously discussed. DGCC total
615 counts were normalised to the chemically similar PC internal standard for quantification of
616 experimental samples: $Counts_{DGCC}/Counts_{PC} = 18.594 \times Quantity_{DGCC}$. Highly linear over this
617 range ($R^2 = 0.992$).

618

619 **Untargeted UPLC-ESI-AutoMS^2 Analysis**

620 UPLC-ESI-AutoMS^2 analysis was performed on a Dionex UltiMate 3000 UPLC system
621 coupled to a Bruker maXis 3G quadrupole - time of flight (Q-ToF) mass spectrometer with
622 an electrospray ionisation source. Lipid samples were dissolved in methanol (200 µL) prior to
623 analysis. A 20 µL injection was taken by autosampler from vials in a cooled sample tray at
624 5°C. The sample was then chromatographically separated over 30 minutes with a Waters
625 Acquity UPLC BEH C8, 1.7 µm particle, 2.1 x 100mm column. A constant flow rate of 0.3
626 mL min^{-1} was used resulting in back pressures of between 260 and 460 bar.

627 Eluent A was water with 0.2% formic acid and 1% 1M ammonium acetate, eluent B
628 was methanol with 0.2% formic acid and 1% 1M ammonium acetate. The column was heated

629 to 50°C and the eluent cooled to 21°C post-column, throughout the analysis. The following
630 multi-step linear gradient was applied, with a constant flow rate of 0.3 mL minute^{-1}: 35%
631 eluent B at 0 minutes, increasing to 80% eluent B at 2 minutes, increasing to 95% eluent B at
632 12 minutes and holding for a further 18 minutes until the end of the run. Eluent B was
633 decreased to 35% over 0.5 minutes post run and the column allowed to equilibrate for 4.5
634 minutes prior to the next run.

635 The mass spectrometer was calibrated by direct infusion of sodium formate solution
636 prior to use (10 mM sodium hydroxide + 0.2% formic acid in 1:1 isopropanol/water). The
637 observed mass accuracy was 0.4 ppm, determined from the standard deviation from the
638 quadratic calibration curve for calibrant ions up to 1000 Da, in positive ion mode. The Q-ToF
639 mass spectrometer yielded a mass resolving power of 21463.70, determined from full width
640 at half maximum (FWHM) of the internal standard peak dilauroylphosphatidylcholine at
641 622.4470 Da [M+H]+ in positive ion mode. Full scan MS was acquired in positive and
642 negative mode between 30 and 1500 Da.

643 During each run (positive and negative ion mode require separate analytical runs) ions
644 above the noise level threshold were subjected to data dependant MS^2 fragmentation. The
645 threshold was set at 2000 and 1000 counts in positive and negative ion mode respectively.
646 Ions with a mass of between 500 - 1500 and 300 - 1500 Da were subject to MS^2
647 fragmentation in positive and negative ion mode respectively. The most abundant two
648 precursor ions eluting during an MS scan were fragmented and after two MS^2 spectra were
649 acquired for a given ion, they were actively excluded from further MS^2 for 1 minute.
650 Fragmentation for MS^2 was achieved by collision induced dissociation (CID) by impact with
651 Argon gas, with stepped collision energies for precursor ions of increasing mass. Ions of 300-
652 500, 500-800 and 800+ Da were fragmented with collision energies of 25, 40 and 50 eV
653 respectively in positive ion mode and 25, 30 and 40 eV in negative ion mode.

654

655 **Untargeted Data Processing**

656 Bruker CompassXport was used to export the raw data prior to processing with the MZMine
657 2 software package (55). MZMine was used to generate extracted ion chromatograms and
658 match these chromatograms between different samples. Integrated peak areas were
659 normalised to the total number of cells extracted and adjusted for recovery of the internal
660 standard (dilauroylglycerophosphatidylcholine). Peak assignments were based upon matching
661 to an extensive, accurate mass, structure query language (SQL) lipid database generated in
662 house. The database was populated by permutations of fatty acids (chain length/degree of
663 unsaturation) and common glycerolipids/sphingolipids. The complete LIPID MAPS (version
664 20130306) structural database (56) and MaConDa mass spectrometry contaminants database
665 (57) were also included.

666 The chemical formulae of database entries were then used to calculate accurate mass
667 m/z values based upon a list of common molecular ion adducts in ESI-MS (58). Tentative
668 assignments were made by matching precursor mass ions with the theoretical database to
669 within a mass difference of < ±10 ppm. Database assignments were then confirmed by the
670 identification of supporting MS2 fragments in each case. Fragments were assigned within a
671 tolerance of < ±20 ppm unless otherwise stated.

672 The MS2 data was assigned using an in house visual basic macro, matching fragment
673 ions to a database of common and diagnostic fragments and dynamically generated neutral
674 losses. Matches were made based upon a tolerance of < 20 ppm (unless otherwise specified).

675

676

Acknowledgements

The authors would like to acknowledge John R. Gittins, Stephanie Tweed, Sophie Richier, Mark Stinchcombe and Victoria Goss for methodological assistance. We thank Benjamin van Mooy and Helen Fredricks (Woods Hole Oceanographic Institution, U.S.A.) for providing the DGCC standard. This work was funded by the University of Southampton - Vice Chancellors Scholarship Award. The purchase of the mass spectrometers was supported by the Wellcome Trust (Grant 057405).

Author Contributions

Jonathan E. Hunter designed the experiments, developed methods, carried out culturing, sample preparation, analysis, data interpretation and wrote the manuscript. The remaining co-authors assisted with experimental design, analysis, interpretation and drafting the manuscript.

689 **References**

690 1. Hoek C, Mann DG, Jahns HM. 1995. Algae. Cambridge University Press.

691 2. Vance JE, Vance DE. 2008. Biochemistry of Lipids, Lipoproteins and Membranes.
692 Elsevier.

693 3. Fahy E, Subramaniam S, Brown HA, Glass CK, Merrill AH, Murphy RC, Raetz CRH,
694 Russell DW, Seyama Y, Shaw W, Shimizu T, Spener F, van Meer G, VanNieuwenhze
695 MS, White SH, Witztum JL, Dennis EA. 2005. A comprehensive classification system
696 for lipids. J Lipid Res 46:839–862.

697 4. Levitan O, Dinamarca J, Hochman G, Falkowski PG. 2014. Diatoms: a fossil fuel of
698 the future. Trends Biotechnol 32:117–124.

699 5. Wakeham SG, Hedges JI, Lee C, Peterson ML, Hernes PJ. 1997. Compositions and
700 transport of lipid biomarkers through the water column and surficial sediments of the
701 equatorial Pacific Ocean. Deep Sea Res Part II Top Stud Oceanogr 44:2131–2162.

702 6. Liebisch G, Vizcaíno JA, Köfeler H, Trötzmüller M, Griffiths WJ, Schmitz G, Spener
703 F, Wakelam MJO. 2013. Shorthand notation for lipid structures derived from mass
704 spectrometry. J Lipid Res 54:1523–1530.

705 7. Benning C, Huang ZH, Gage DA. 1995. Accumulation of a novel glycolipid and a
706 betaine lipid in cells of Rhodobacter sphaeroides grown under phosphate limitation.
707 Arch Biochem Biophys 317:103–11.

708 8. Martin P, Van Mooy BAS, Heithoff A, Dyhrman ST. 2011. Phosphorus supply drives
709 rapid turnover of membrane phospholipids in the diatom Thalassiosira pseudonana.
710 ISME J 5:1057–1060.

711 9. Van Mooy BAS, Fredricks HF, Pedler BE, Dyhrman ST, Karl DM, Koblížek M,
712 Lomas MW, Mincer TJ, Moore LR, Moutin T, Rappé MS, Webb EA. 2009.
713 Phytoplankton in the ocean use non-phosphorus lipids in response to phosphorus
714 scarcity. Nature 458:69–72.

715 10. Van Mooy BAS, Rocap G, Fredricks HF, Evans CT, Devol AH. 2006. Sulfolipids
716 dramatically decrease phosphorus demand by picocyanobacteria in oligotrophic marine
717 environments. Proc Natl Acad Sci 103:8607–8612.

718 11. Thingstad TF. 2005. Nature of Phosphorus Limitation in the Ultraoligotrophic Eastern
719 Mediterranean. Science 309:1068–1071.

720 12. Mather RL, Reynolds SE, Wolff GA, Williams RG, Torres-Valdes S, Woodward EMS,
721 Landolfi A, Pan X, Sanders R, Achterberg EP. 2008. Phosphorus cycling in the North
722 and South Atlantic Ocean subtropical gyres. Nat Geosci 1:439–443.

723 13. Guschina IA, Harwood JL. 2006. Lipids and lipid metabolism in eukaryotic algae.
724 Prog Lipid Res 45:160–186.

725 14. Eichenberger W, Gribi C. 1997. Lipids of Pavlova lutheri: Cellular site and metabolic
726 role of DGCC. Phytochemistry 45:1561–1567.

727 15. Schubotz F, Wakeham SG, Lipp JS, Fredricks HF, Hinrichs K-U. 2009. Detection of
728 microbial biomass by intact polar membrane lipid analysis in the water column and
729 surface sediments of the Black Sea. Environ Microbiol 11:2720–34.

730 16. Van Mooy BAS, Fredricks HF. 2010. Bacterial and eukaryotic intact polar lipids in the
731 eastern subtropical South Pacific: Water-column distribution, planktonic sources, and
732 fatty acid composition. Geochim Cosmochim Acta 74:6499–6516.

733 17. Popendorf, Tanaka T, Pujo-Pay M, Lagaria A, Courties C, Conan P, Oriol L, Sofen LE,
734 Moutin T, Van Mooy BAS. 2011. Gradients in intact polar diacylglycerolipids across
735 the Mediterranean Sea are related to phosphate availability. Biogeosciences 8:3733–
736 3745.

737 18. Brandsma J, Hopmans EC, Philippart CJM, Veldhuis MJW, Schouten S, Sinninghe
738 Damsté JS. 2012. Low temporal variation in the intact polar lipid composition of North
739 Sea coastal marine water reveals limited chemotaxonomic value. Biogeosciences
740 9:1073–1084.

741 19. Bellinger BJ, Van Mooy BAS, Cotner JB, Fredricks HF, Benitez-Nelson CR,
742 Thompson J, Cotter A, Knuth ML, Godwin CM. 2014. Physiological modifications of
743 seston in response to physicochemical gradients within Lake Superior. Limnol
744 Oceanogr 59:1011–1026.

745 20. Lykidis A. 2007. Comparative genomics and evolution of eukaryotic phospholipid
746 biosynthesis. Prog Lipid Res 46:171–199.

747 21. Riekhof WR, Sears BB, Benning C. 2005. Annotation of Genes Involved in

748 Glycerolipid Biosynthesis in Chlamydomonas reinhardtii: Discovery of the Betaine
749 Lipid Synthase BTA1Cr. Eukaryot Cell 4:242–252.

750 22. Sato N. 1988. Dual Role of Methionine in the Biosynthesis of
751 Diacylglyceryltrimethylhomoserine in Chlamydomonas reinhardtii. Plant Physiol
752 86:931–934.

753 23. Vogel G, Eichenberger W. 1992. Betaine Lipids in Lower Plants. Biosynthesis of
754 DGTS and DGTA in Ochromonas danica (Chrysophyceae) and the Possible Role of
755 DGTS in Lipid Metabolism. Plant Cell Physiol 33:427–436.

756 24. Armbrust EV. 2004. The Genome of the Diatom Thalassiosira Pseudonana: Ecology,
757 Evolution, and Metabolism. Science 306:79–86.

758 25. Kato M, Kobayashi Y, Torii A, Yamada M. 2003. Betaine Lipids in Marine Algae, p.
759 19–22. *In* Murata, N, Yamada, M, Nishida, I, Okuyama, H, Sekiya, J, Hajime, W
760 (eds.), Advanced Research on Plant Lipids SE - 3. Springer Netherlands.

761 26. Mizusawa N, Wada H. 2012. The role of lipids in photosystem II. Biochim Biophys
762 Acta - Bioenerg 1817:194–208.

763 27. Abida H, Dolch L-J, Meï C, Villanova V, Conte M, Block MA, Finazzi G, Bastien O,
764 Tirichine L, Bowler C, Rébeillé F, Petroutsos D, Jouhet J, Maréchal E. 2015.
765 Membrane Glycerolipid Remodeling Triggered by Nitrogen and Phosphorus
766 Starvation in Phaeodactylum tricornutum. Plant Physiol 167:118–136.

767 28. Shemi A, Schatz D, Fredricks HF, Mooy BAS Van, Porat Z, Vardi A. 2016.
768 Acclimation to phosphorus starvation is mediated by membrane remodeling and
769 recycling in a bloom-forming coccolithophore. New Phytol.

770 29. Brandsma J. 2016. Phytoplankton phenotype plasticity induced by phosphorus
771 starvation may play a significant role in marine microbial ecology and
772 biogeochemistry. New Phytol 211:765–766.

773 30. Dyhrman ST, Jenkins BD, Rynearson TA, Saito MA, Mercier ML, Alexander H,
774 Whitney LP, Drzewianowski A, Bulygin V V, Bertrand EM, Wu Z, Benitez-Nelson C,
775 Heithoff A. 2012. The Transcriptome and Proteome of the Diatom Thalassiosira
776 pseudonana Reveal a Diverse Phosphorus Stress Response. PLoS One 7:e33768.

777 31. Núñez-Milland DR, Baines SB, Vogt S, Twining BS. 2010. Quantification of

778 phosphorus in single cells using synchrotron X-ray fluorescence. J Synchrotron Radiat
779 17:560–566.

780 32. Brembu T, Mühlroth A, Alipanah L, Bones AM. 2017. The effects of phosphorus
781 limitation on carbon metabolism in diatoms. Philos Trans R Soc B Biol Sci
782 372:20160406.

783 33. Von Dassow P, Petersen TW, Chepurnov VA, Virginia Armbrust E. 2008. Inter- and
784 Intraspecific Relationships Between Nuclear DNA Content and Cell Size in Selected
785 Members of the Centric Diatom Genus Thalassiosira (Bacillariophyceae). J Phycol
786 44:335–349.

787 34. Martin P, Van Mooy BAS. 2013. Fluorometric Quantification of Polyphosphate in
788 Environmental Plankton Samples: Extraction Protocols, Matrix Effects, and Nucleic
789 Acid Interference. Appl Environ Microbiol 79:273–281.

790 35. Martin P, Dyhrman ST, Lomas MW, Poulton NJ, Van Mooy BAS. 2014.
791 Accumulation and enhanced cycling of polyphosphate by Sargasso Sea plankton in
792 response to low phosphorus. Proc Natl Acad Sci 111:8089–8094.

793 36. Matsumiya Y, Wakita D, Kimura A, Sanpa S, Kubo M. 2007. Isolation and
794 characterization of a lipid-degrading bacterium and its application to lipid-containing
795 wastewater treatment. J Biosci Bioeng 103:325–330.

796 37. Sato N, Sonoike K, Tsuzuk M, Kawaguchi A. 1995. Impaired Photosystem II in a
797 Mutant of Chlamydomonas Reinhardtii Defective in Sulfoquinovosyl Diacylglycerol.
798 Eur J Biochem 234:16–23.

799 38. Hodgson P, Henderson RJ, Sargent J, Leftley J. 1991. Patterns of variation in the lipid
800 class and fatty acid composition of Nannochloropsis oculata (Eustigmatophyceae)
801 during batch culture. J Appl Phycol 3:169–181.

802 39. Dymond MK, Hague C V, Postle AD, Attard GS. 2012. An in vivo ratio control
803 mechanism for phospholipid homeostasis: evidence from lipidomic studies. J R Soc
804 Interface 10:20120854–20120854.

805 40. Lang I, Hodac L, Friedl T, Feussner I. 2011. Fatty acid profiles and their distribution
806 patterns in microalgae: a comprehensive analysis of more than 2000 strains from the
807 SAG culture collection. BMC Plant Biol 11:124.

41. Kato M, Sakai M, Adachi K, Ikemoto H, Sano H. 1996. Distribution of betaine lipids in marine algae. Phytochemistry 42:1341–1345.

42. Popendorf KJ, Lomas MW, Van Mooy BAS. 2011. Microbial sources of intact polar diacylglycerolipids in the Western North Atlantic Ocean. Org Geochem 42:803–811.

43. Zhao F, Xu J, Chen J, Yan X, Zhou C, Li S, Xu X, Ye F. 2013. Structural elucidation of two types of novel glycosphingolipids in three strains of Skeletonema by liquid chromatography coupled with mass spectrometry. Rapid Commun Mass Spectrom 27:1535–1547.

44. Pata MO, Hannun YA, Ng CK-Y. 2010. Plant sphingolipids: decoding the enigma of the Sphinx. New Phytol 185:611–630.

45. Vardi A, Van Mooy BAS, Fredricks HF, Popendorf KJ, Ossolinski JE, Haramaty L, Bidle KD. 2009. Viral glycosphingolipids induce lytic infection and cell death in marine phytoplankton. Science 326:861–5.

46. Vardi A, Haramaty L, Van Mooy BAS, Fredricks HF, Kimmance SA, Larsen A, Bidle KD. 2012. Host–virus dynamics and subcellular controls of cell fate in a natural coccolithophore population. Proc Natl Acad Sci 109:19327–19332.

47. Hunter JE, Frada MJ, Fredricks HF, Vardi A, Van Mooy BAS. 2015. Targeted and untargeted lipidomics of Emiliania huxleyi viral infection and life cycle phases highlights molecular biomarkers of infection, susceptibility, and ploidy. Front Mar Sci 2.

48. Fulton JM, Fredricks HF, Bidle KD, Vardi A, Kendrick BJ, DiTullio GR, Van Mooy BAS. 2014. Novel molecular determinants of viral susceptibility and resistance in the lipidome of Emiliania huxleyi. Environ Microbiol 16:1137–1149.

49. Guillard RRL. 1975. Culture of phytoplankton for feeding marine invertebrates., p. 22–60. *In* Smith, WL, Chanley, MH (eds.), Culture of Marine Invertebrate Animals. Plenum Press, New York, USA.

50. Kester DR, Duedall IW, Connors DN, Pytkowicz RM. 1967. Preparation of Artificial Seawater. Limnol Oceanogr 12:176–179.

51. Raimbault P, Diaz F, Pouvesle W, Boudjellal B. 1999. Simultaneous determination of particulate organic carbon, nitrogen and phosphorus collected on filters, using a semi-

automatic wet-oxidation method. Mar Ecol Prog Ser 180:289–295.

52. Bligh EG, Dyer WJ. 1959. A Rapid Method of Total Lipid Extraction and Purification. Can J Biochem Physiol 37:911–917.

53. Popendorf KJ, Fredricks HF, Van Mooy BAS. 2013. Molecular Ion-Independent Quantification of Polar Glycerolipid Classes in Marine Plankton Using Triple Quadrupole MS. Lipids 48:185–195.

54. Postle AD, Henderson NG, Koster G, Clark HW, Hunt AN. 2011. Analysis of lung surfactant phosphatidylcholine metabolism in transgenic mice using stable isotopes. Chem Phys Lipids 164:549–555.

55. Pluskal T, Castillo S, Villar-Briones A, Orešič M. 2010. MZmine 2: Modular framework for processing, visualizing, and analyzing mass spectrometry-based molecular profile data. BMC Bioinformatics 11:395.

56. Sud M, Fahy E, Cotter D, Brown A, Dennis EA, Glass CK, Merrill AH, Murphy RC, Raetz CRH, Russell DW, Subramaniam S. 2007. LMSD: LIPID MAPS structure database. Nucleic Acids Res 35:D527–D532.

57. Weber RJM, Li E, Bruty J, He S, Viant MR. 2012. MaConDa: a publicly accessible mass spectrometry contaminants database. Bioinformatics 28:2856–2857.

58. Huang N, Siegel MM, Kruppa GH, Laukien FH. 1999. Automation of a Fourier transform ion cyclotron resonance mass spectrometer for acquisition, analysis, and e-mailing of high-resolution exact-mass electrospray ionization mass spectral data. J Am Soc Mass Spectrom 10:1166–1173.

861 **Figure Legends**

862 *Figure 1: Cell concentration growth curve (A); particulate organic phosphorus (POP) per*
863 *cell (B); Total phospholipid (P-Lipid, C); total DGCC (D) and the quantity of non-lipidic*
864 *POP per cell (E) in the phosphorus replete (P+) and phosphorus stressed (P-) cultures,*
865 *under P+ and P- conditions, with the progression of time. Panel (F) depicts the loss rate of*
866 *the total phospholipids (P-Lipid) in comparison with the cell dilution rate. Values are relative*
867 *to 12 h, observed as the initiation of P stress and consequently DGCC biosynthesis and P-*
868 *Lipid substitution/degradation in the P- cultures. Data are the mean of three biological*
869 *replicates, with shaded error regions of one standard deviation.*

870

871 *Figure 2: Individual lipid molecular species quantity per cell within each of the lipid classes*
872 *measured at 72 h in the P+ and P- cultures. [α]All quantities are in amol cell^{-1} with the*
873 *exception of MGDG (G) and DGDG (H), for which relative, percentage abundances are*
874 *shown. Molecular species contributing less than 5% of the total quantity in their lipid head*
875 *group class in both treatments were excluded for brevity. The predominant fatty acyl*
876 *combinations are shown where identified and consistent across the present lipids. Data are*
877 *the mean of three biological replicates, with error bars of one standard deviation. Statistical*
878 *significance is indicated in the figure and accompanying text, *$p<0.05$ **$p<0.005$ by two-*
879 *tailed, paired equal-variance T-test.*

880

881 *Figure 3 – Top 5 most abundant individual PC lipid molecular species quantity per cell,*
882 *through time, in the P+ control cultures only (A), change in the top 5 PC lipid molecular*
883 *species, between time (t) and the initiation of P stress (12 h) in the P- cultures only (B) and*
884 *the average unsaturation of the total PC lipid pool in P+ and P- treatments, with the*

885 *progression of time (C). Data are the mean of three biological replicates, with shaded error*
886 *regions of one standard deviation.*

887

888 *Figure 4 – Untargeted lipidomic screening determined a total of 1161 different molecular*
889 *ions in the 72 h P+ and P- cultures using positive and negative ion mass spectrometry. The*
890 *normalised abundance in the P- cultures, indicating how strongly a given ion was associated*
891 *with the P stressed cultures, is plotted against mass to charge ratio (m/z) and*
892 *chromatographic retention time (R.T.) in panel (A). The top 15 ions associated with the P*
893 *stressed cultures in positive and negative mode identified where possible by database*
894 *matching and MS2 fragmentation analysis are shown in panel (B).*

895

896 *Figure 5 - Fold change, subject to P stress, in observed ions related to* $(Gly)_2Cer(d18:3/24:0)$,
897 *in positive ion mode. Long chain base and fatty acid amide fragments were observed in*
898 *support of each of the following assignments in positive MS2. Data represent the mean of*
899 *biological triplicate samples with error bars of one standard deviation. Assignments*
900 *represent the primary fatty acyl configuration, as determined by the abundance of the fatty*
901 *acyl fragments in the MS2 spectra.*

902

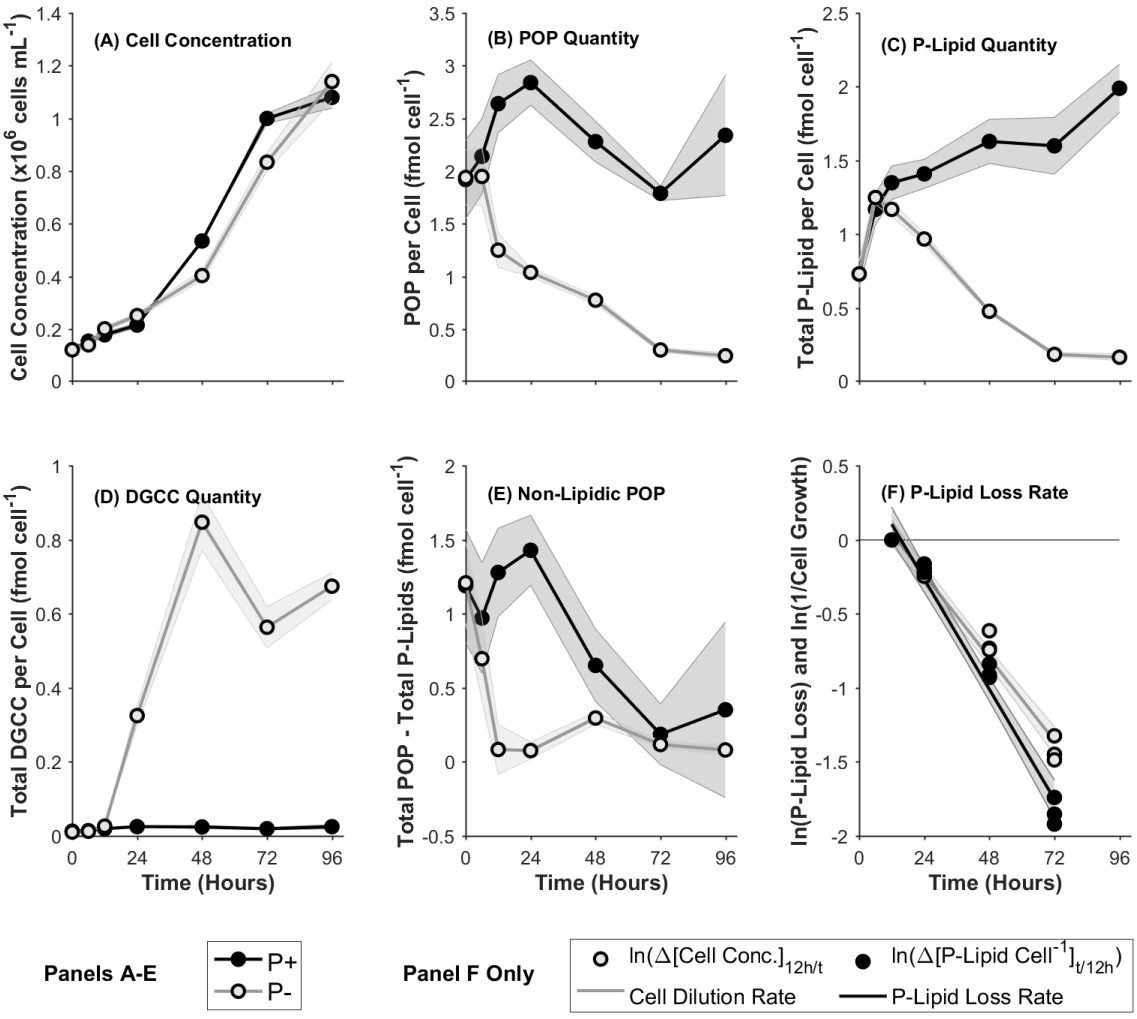

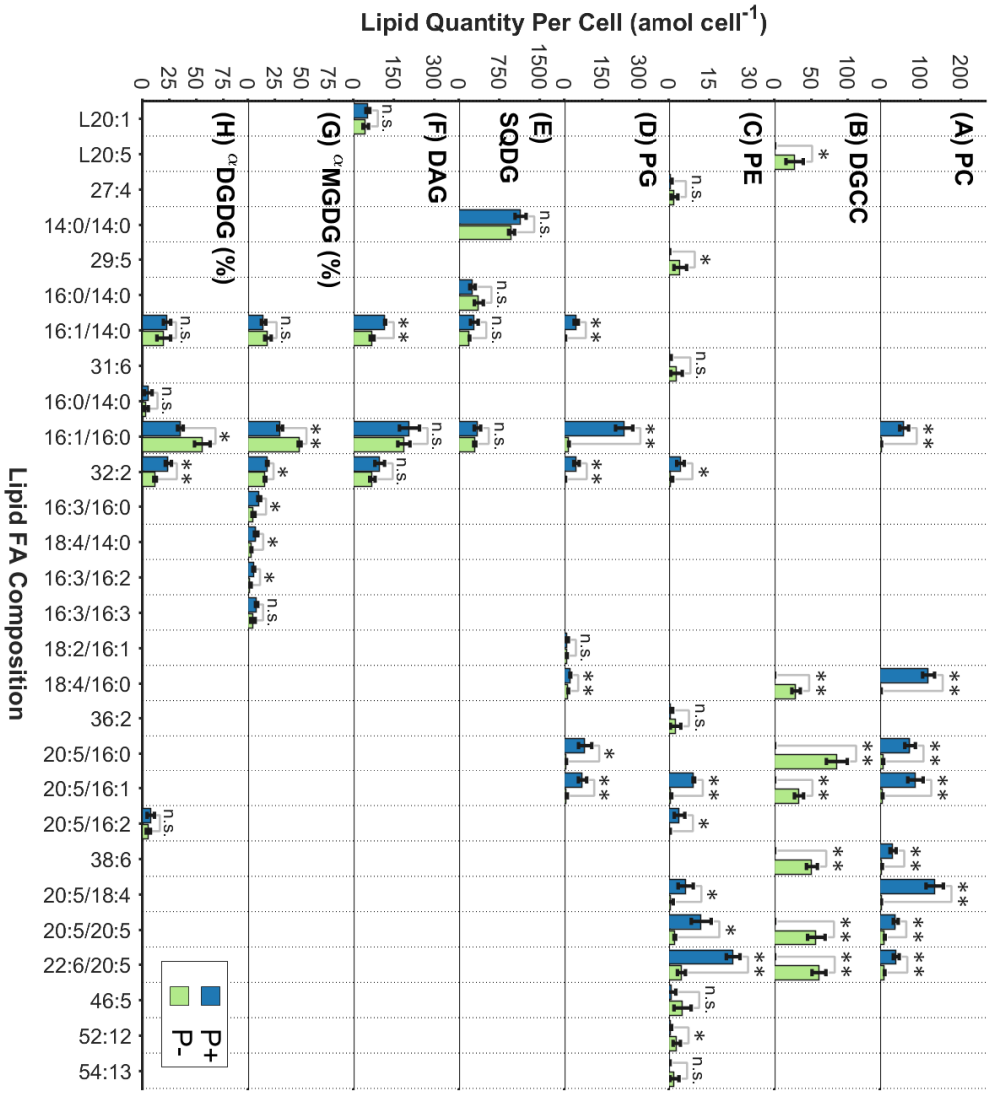

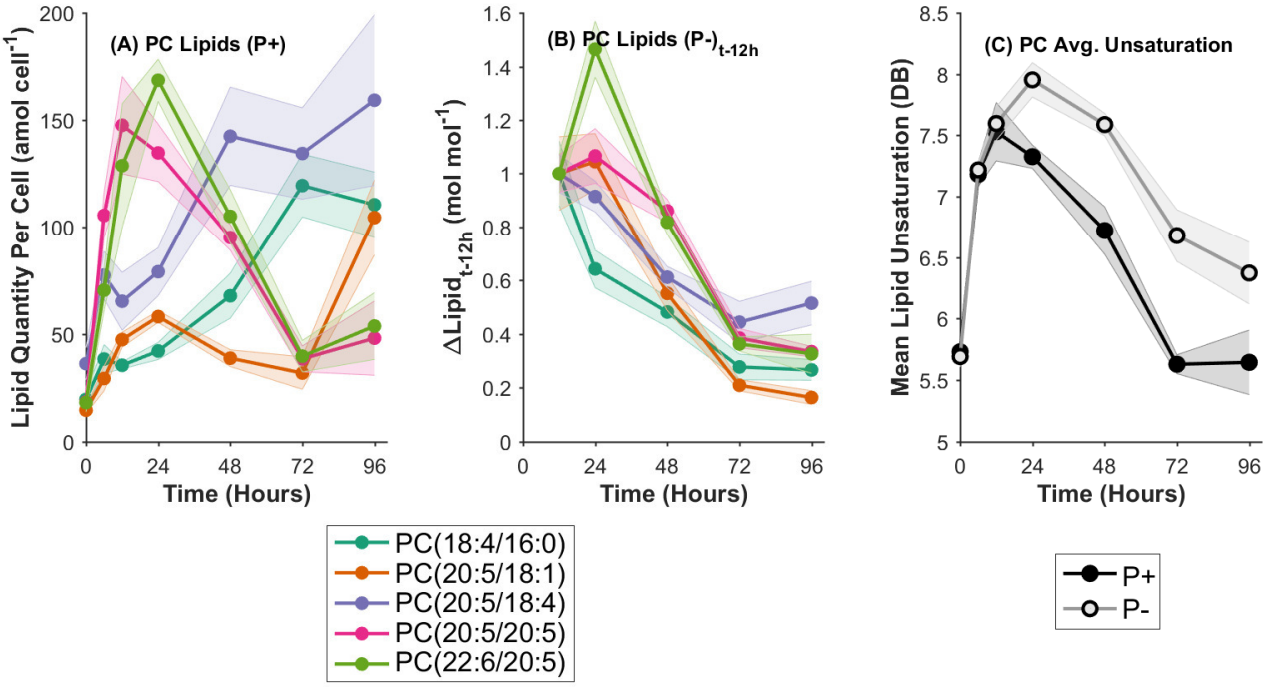

(A) Lipids highly indicative of P- (in positive and negative ion mode):

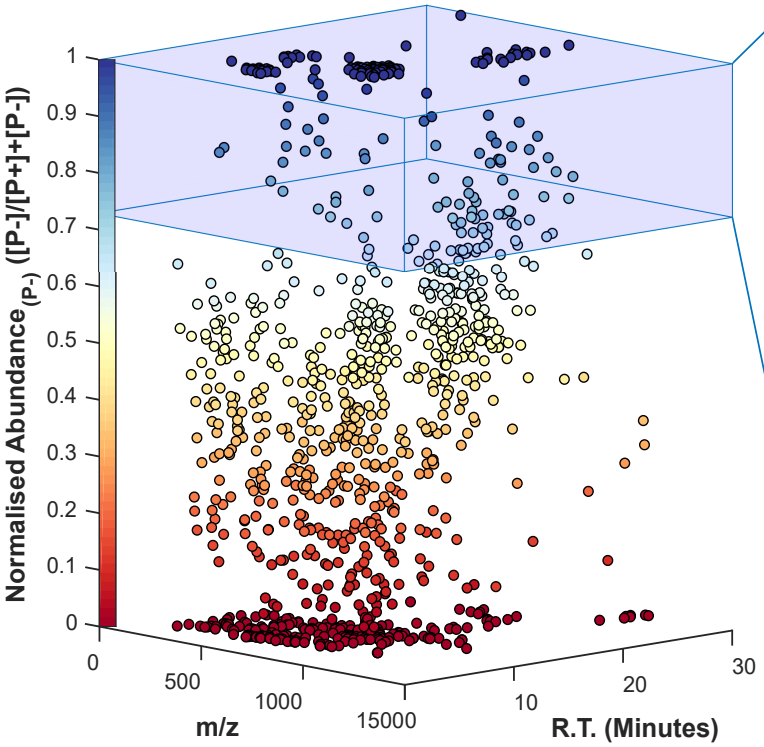

(B) Lipid ID	Mode	Normalised Abundance
DGCC(20:5/16:0)	+,-	1.00
LDGCC(20:5)	+	1.00
DGCC(22:6/16:0)	+,-	1.00
LDGCC(22:6)	+	1.00
DGCC(20:5/20:5)	+	1.00
DGCC(22:6/20:5)	+,-	1.00
DGCC(20:5/16:1)	+,-	1.00
DGCC(18:4/16:0)	+,-	1.00
DGCC(16:1/16:0)	+,-	1.00
DGCC(20:5/14:0)	+	1.00
LDGCC(18:4)	+	1.00
DGCC(16:1/16:1)	+	1.00
TAG(16:0/16:0/14:0)	+	1.00
DGCC(20:5/18:2)	+	1.00
DGCC(20:5/18:4)	+,-	1.00
Unknown	-	1.00
$(Gly)_2Cer(d18:3/24:0)$	-	1.00
LDGCC(16:1)	-	1.00
DGCC(18:2/16:0)	-	1.00
Unknown	-	1.00
Unknown	-	0.86
SQDG(34:1)	-	0.78
Unknown	-	0.73